**AST 853** **Numerical Weather Prediction** Dr. Yuh-Lang Lin
Department of Energy & Environmental Systems ylin@ncat.edu
North Carolina A&T State University http://mesolab.org

# NWP Lecture 2 (Lin 2007 Ch. 2)

## Ch. 2 Lecture Note: Governing Equations of Stratified and Shallow-Water Flow

(Based on Ch. 2 & 3, "Mesoscale Dynamics" by Y.-L. Lin 2007)

## 2.1 Introduction

- The governing equations are based on:

  (a) Newton's second law,

  (b) Conservation of mass, and

  (c) Conservation of energy.

- The above conservation laws are represented by the horizontal and vertical equations of motion, continuity equation, and the thermodynamic energy equation, respectively.

## 2.2 Governing Equations of Mesoscale Stratified Fluid Flow

The momentum equations, continuity equation, and thermodynamic energy equation governing an atmospheric fluid flow can be expressed as,

$$\frac{Du}{Dt} - fv = -\frac{1}{\rho}\frac{\partial p}{\partial x} + F_{rx}, \qquad (2.2.1)$$

$$\frac{Dv}{Dt} + fu = -\frac{1}{\rho}\frac{\partial p}{\partial y} + F_{ry}, \qquad (2.2.2)$$

$$\frac{Dw}{Dt} = -\frac{1}{\rho}\frac{\partial p}{\partial z} - g + F_{rz}, \qquad (2.2.3)$$

$$\frac{D\rho}{Dt} + \rho\left(\frac{\partial u}{\partial x} + \frac{\partial v}{\partial y} + \frac{\partial w}{\partial z}\right) = 0, \qquad (2.2.4)$$

$$\frac{D\theta}{Dt} = \frac{\theta}{c_p T} q + F_{\theta}, \qquad (2.2.5)$$

where $D/Dt = \partial/\partial t + u\partial/\partial x + v\partial/\partial y + w\partial/\partial z$ is the *total* or *material derivative*, which represents the change of a certain property within a fluid parcel following the motion, $F_{rx}, F_{ry},$ and $F_{rz}$ are the viscous terms in *x*, *y*, and *z* directions, respectively.

- Earth curvature terms need to be considered for large scale motions, which are often incorporated in NWP models. See Holton (2012) for details.

- The friction and heat fluxes (e.g., sensible heat and latent heat) associated with planetary boundary layer (PBL) processes are normally parameterized by the $F_r$ and $F_\theta$ terms, respectively in a numerical model. This proposes a challenging problem in NWP or mesoscale modeling.

- The diabatic heating rate ($q$) represent the surface heating, elevated latent heating and radiative heating rate per unit mass. Accurate parameterizations of these processes are essential for successful NWP.

- Representations of the diabatic heating in NWP models:

(a) The surface heating and friction is part of the PBL processes, thus is usually represented by PBL parameterization and land surface parameterization schemes.

(b) The latent heating is represented by cumulus parameterization schemes (subgrid) or microphysical parameterization (grid explicit) schemes.

(c) The radiative processes are represented by longwave and shortwave radiation (radiative transfer) parameterization schemes.

- The equation set (2.2.1)-(2.2.3) is often referred to as the *Navier-Stokes equations of motion*.

- Some basic dynamics can be learned by studying the perturbation equations, which neglect the nonlinear (e.g., $u'\partial u'/\partial x$) and viscosity terms,

$$\frac{\partial u'}{\partial t}+U\frac{\partial u'}{\partial x}+V\frac{\partial u'}{\partial y}+U_z w'-fv'+\frac{1}{\bar{\rho}}\frac{\partial p'}{\partial x}=0\,, \tag{2.2.12}$$

$$\frac{\partial v'}{\partial t}+U\frac{\partial v'}{\partial x}+V\frac{\partial v'}{\partial y}+V_z w'+fu'+\frac{1}{\bar{\rho}}\frac{\partial p'}{\partial y}=0\,, \tag{2.2.13}$$

$$\frac{\partial w'}{\partial t}+U\frac{\partial w'}{\partial x}+V\frac{\partial w'}{\partial y}-g\frac{\theta'}{\bar{\theta}}+\frac{1}{\bar{\rho}}\frac{\partial p'}{\partial z}+\frac{p'}{\bar{\rho}H}=0\,, \tag{2.2.14}$$

$$\frac{1}{c_s^2}\left(\frac{\partial p'}{\partial t}+U\frac{\partial p'}{\partial x}+V\frac{\partial p'}{\partial y}\right)-\frac{\bar{\rho}}{H}w'+\bar{\rho}\nabla\cdot\boldsymbol{V}'=\frac{\bar{\rho}}{c_p\bar{T}}q'\,, \tag{2.2.15}$$

$$\frac{\partial \theta'}{\partial t} + U\frac{\partial \theta'}{\partial x} + V\frac{\partial \theta'}{\partial y} + \frac{N^2\overline{\theta}}{g}w' = \frac{\overline{\theta}}{c_p\overline{T}}q', \qquad (2.2.16)$$

where $N$ is the Brunt-Vaisala (buoyancy) frequency and H is the scale height, which are defined as

$$N^2 \equiv \frac{g}{\overline{\theta}}\frac{\partial \overline{\theta}}{\partial z}, \qquad H \equiv \frac{c_s^2}{g}$$

$$c_s^2 = \gamma R\overline{T}, \quad \text{and} \quad \gamma = \frac{c_p}{c_v}. \qquad (2.2.17)$$

## 2.3 Approximations to the Governing Equations

➢ *Three forms of the continuity equation are often used in the literature.*

***(a)*** ***Fully compressible continuity equation:*** (2.2.4)

One of the advantage of this system is that the key dependent variables are all predicted (i.e. time dependent), instead of prognostic (time-independent), thus there is no need to make the diagnosis for certain time-independent unknown variables. However, note that sound waves are included in the system, which requires a very small time step (interval) to keep the numerical integration stable and efficient, thus a special treatment of them is necessary.

One popular scheme used in NWP models is the *time-splitting scheme* in which a smaller time step is adopted for simulating the terms related to sound waves while a larger time step is adopted for simulating the other terms in the governing equations.

Most of the popular mesoscale research models, such as WRF (NCAR), MM5 (PSU-NCAR), ARPS (OU), CSU-RAMS, and COAMPS (NRL) models.

***(b) Anelastic or deep convection continuity equation***

$$\nabla \cdot \boldsymbol{V'} - \frac{w'}{H} = 0, \qquad (2.3.1)$$

$$\nabla \cdot (\boldsymbol{V'} e^{-z/H}) = 0, \text{ or} \qquad (2.3.2)$$

$$\nabla \cdot (\bar{\rho} \boldsymbol{V'}) = 0. \qquad (2.3.3)$$

where *H* is the scale height. Since sound waves are filtered in this approximation, there is no need to adopt time-splitting scheme.

***(c) Incompressible or shallow convection continuity equation***

$$\nabla \cdot \boldsymbol{V'} = 0. \qquad (2.3.4)$$

This approximation is valid when $L_z / H \ll 1$. It is important to mention that $L_z$ represents the depth of convection (dry or moist) or motion, while *H* represents the scale height, which is controlled by the basic structure of the atmosphere, instead of the motion.

- A well-known approximation, which has been used widely in theoretical studies, is the *Boussinesq approximation* (Boussinesq 1903), which is equivalent to that: (1) $1/L_z \gg 1/H$, (2) density is treated as a constant except where it is coupled to gravity in the buoyancy term of the vertical momentum equation, and (3) replace $\bar{\rho}$ and $\bar{\theta}$ by $\rho_o$ and $\theta_o$, respectively.

- For a disturbance with a much larger horizontal scale than vertical scale, the vertical acceleration generally becomes small and may be neglected. This leads to the *hydrostatic equation*,

$$\frac{\partial p}{\partial z} = -\rho g \qquad (2.3.12)$$

Or the *linear hydrostatic equation*,

$$\frac{\partial p'}{\partial z} - \left(\frac{g\bar{\rho}}{\bar{\theta}}\right)\theta' = 0 . \qquad (2.3.12)'$$

In the pressure coordinates, the hydrostatic, Boussinesq equations can be written (Emanuel and Raymond 1984)

$$\frac{D\boldsymbol{V}'}{Dt} + \nabla\phi' + f\boldsymbol{k} \times \boldsymbol{V}' = 0 \qquad (2.3.15)$$

$$\frac{d\phi'}{dp} = -\frac{1}{\rho_o}\left(\frac{p_o}{p}\right)^{1/\gamma} e^{b'/g} , \qquad (2.3.16)$$

$$\frac{\partial u'}{\partial x} + \frac{\partial v'}{\partial y} + \frac{\partial \omega}{\partial p} = 0 , \qquad (2.3.17)$$

$$\frac{Db'}{Dt} = 0 , \qquad (2.3.18)$$

where

$\boldsymbol{V}' = (u', v')$, $\phi' = gz =$ perturbation geopotential, $\omega = Dp/Dt$, $p_o$ and $\rho_o$ are constant reference pressure and density, respectively, and $b' = g\theta'/\theta_o$ is the perturbation buoyancy.

- Note that in some NWP models, a vertical pressure coordinate, instead of a height coordinate is adopted. In order to incorporate the terrain into the model, $\sigma - p$ and $\sigma - z$ coordinates have been introduced.

- Also, some NWP models adopt the Exner function to replace the pressure in their model equations. The *Exner function* is defined as

$$\pi \equiv c_p \left( \frac{p}{p_o} \right)^{R_d / c_p} .$$

In some models or papers, the *Exner function* is defined as

$$\pi \equiv \left( \frac{p}{p_o} \right)^{R_d / c_p} .$$

This may be called *nondimensional Exner function*.

## 2.4 Shallow Water Wave Equations

(Ref.: Sec. 3.4 of Lin 2007)

- Consider a
  (1) non-rotating ($f$ = 0),
  (2) hydrostatic,
  (3) two-layer fluid system with constant densities $\rho_1$ and $\rho_o$ in the upper and lower layers, respectively, (Fig. 3.2) and
  (4) $\rho_1 < \rho_o$, the pressure gradients at the interface can be approximated by

$$\frac{\partial p}{\partial x} = g\Delta\rho \frac{\partial (h+h_s)}{\partial x},$$
$$\frac{\partial p}{\partial y} = g\Delta\rho \frac{\partial (h+h_s)}{\partial y},$$

where $\Delta\rho = \rho_o - \rho_1$ and $h_s$ is the height of the topography (see Fig. 3.2). The above equations can be understood by considering flow over a flat terrain or bottom topography, $h_s = 0$, by considering the fluid is in hydrostatic balance.

In deriving the above equations, we have used $h+h_s=H+h'$, where $h$ is the depth of the fluid.

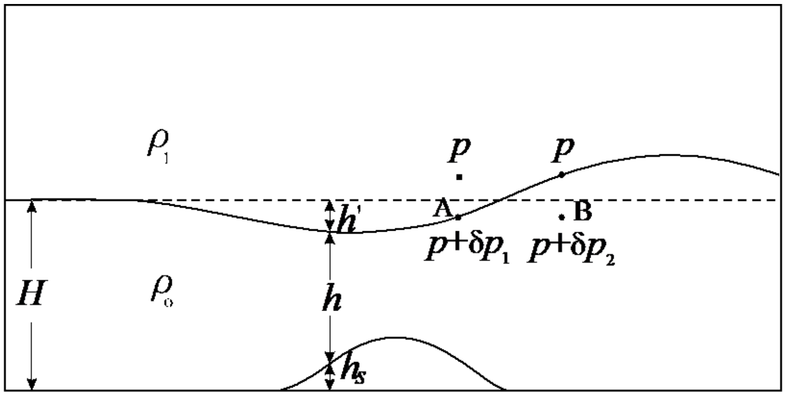


Fig. 3.2: A two-layer system of homogeneous fluids. Symbols $H$, $h$, $h_s$, and $h'$ denote the undisturbed fluid depth, actual fluid depth, bottom topography, and perturbation (vertical displacement) from the undisturbed fluid depth, respectively. The densities of the upper and lower layers are $\rho_1$ and $\rho_o$, respectively. The pressure perturbations at A and B from $p$ in the upper layer are denoted by $p+\delta p_1$ and $p+\delta p_2$, respectively. (From Lin 2007)

- By assuming no initial vertical shear, the horizontal momentum equations become

$$\frac{\partial u}{\partial t} + u\frac{\partial u}{\partial x} + v\frac{\partial u}{\partial y} = -g'\frac{\partial (h+h_s)}{\partial x}, \tag{3.4.1}$$

$$\frac{\partial v}{\partial t}+u\frac{\partial v}{\partial x}+v\frac{\partial v}{\partial y}=-g'\frac{\partial(h+h_s)}{\partial y}, \qquad (3.4.2)$$

where $g'=g\Delta\rho/\rho_o$ is the *reduced gravity*.

- The continuity equation in a shallow water system can be derived,

$$\frac{\partial h}{\partial t}+u\frac{\partial h}{\partial x}+v\frac{\partial h}{\partial y}+h\left(\frac{\partial u}{\partial x}+\frac{\partial v}{\partial y}\right)=0, \qquad (3.4.3)$$

One may substitute $u=U+u'$, $v=V+v'$, and $h=H+h'-h_s$ to obtain the perturbation form,

$$\frac{\partial u'}{\partial t}+(U+u')\frac{\partial u'}{\partial x}+(V+v')\frac{\partial u'}{\partial y}+g'\frac{\partial h'}{\partial x}=0, \qquad (3.4.4)$$

$$\frac{\partial v'}{\partial t}+(U+u')\frac{\partial v'}{\partial x}+(V+v')\frac{\partial v'}{\partial y}+g'\frac{\partial h'}{\partial y}=0, \qquad (3.4.5)$$

$$\frac{\partial h'}{\partial t}+(U+u')\frac{\partial h'}{\partial x}+(V+v')\frac{\partial h'}{\partial y}+(H+h'-h_s)\left(\frac{\partial u'}{\partial x}+\frac{\partial v'}{\partial y}\right)$$
$$=(U+u')\frac{\partial h_s}{\partial x}+(V+v')\frac{\partial h_s}{\partial y}. \qquad (3.4.6)$$

- [Special Case - 2D ($x$, $z$), linear, one-layer system] The governing equations for two-dimensional, small-perturbation (linear), one-layered fluid system with a flat bottom reduce to the following

$$\frac{\partial u'}{\partial t}+U\frac{\partial u'}{\partial x}+g\frac{\partial h'}{\partial x}=0, \qquad (3.4.7)'$$

$$\frac{\partial h'}{\partial t} + U\frac{\partial h'}{\partial x} + H\frac{\partial u'}{\partial x} = 0. \qquad (3.4.8)'$$

The above two equations may be combined to

$$\left(\frac{\partial}{\partial t} + U\frac{\partial}{\partial x}\right)^2 h' - (gH)\left(\frac{\partial^2 h'}{\partial x^2}\right) = 0. \qquad (3.4.9)'$$

We may obtain the analytical solution (or applying the characteristic equation method) directly from the governing equation,

$$h'(t,x) = \frac{1}{2} f[x + (U + \sqrt{gH})\,t] + \frac{1}{2} f[x + (U - \sqrt{gH})t], \qquad (3.4.12)'$$

where *f* preserves the same shape of the initial disturbance but with the amplitude reduced to half. For example, the shallow-water waves with the initial bell-shaped disturbance

$$h'(x) = \frac{h_o b^2}{x^2 + b^2}\,, \qquad (3.4.13)$$

are represented by,

$$h'(x,t) = \frac{(h_o/2)b^2}{[x + (U + \sqrt{gH})t]^2 + b^2} + \frac{(h_o/2)b^2}{[x + (U - \sqrt{gH})t]^2 + b^2}. \qquad (3.4.14)$$

- The governing equation for a two-dimensional, small-perturbation shallow water fluid flow over an obstacle can be derived,

$$\left(\frac{\partial}{\partial t} + U\frac{\partial}{\partial x}\right)^2 h' - (gH)\frac{\partial^2 h'}{\partial x^2} = U\left(\frac{\partial}{\partial t} + U\frac{\partial}{\partial x}\right)\frac{\partial h_s}{\partial x}\,, \qquad (3.4.16)$$

which gives the following steady state solution

$$h' = \left( \frac{U^2}{U^2 - gH} \right) h_s = \frac{h_s}{1 - F^{-2}} \;; \quad F \equiv \frac{U}{\sqrt{gH}} \qquad (3.4.17)$$

where $F$ is called the ***Froude number***.

Thus, we have

$$h' \propto h_s \qquad \text{for } F > 1,$$
$$h' \propto -h_s \qquad \text{for } F < 1, \qquad (3.4.18)$$

- Froude number is related to the ratio of kinetic energy and potential energy of the upstream basic flow.

Note that in the real atmosphere, ocean, or other geofluid, there is density variation with height (i.e., stratification). Thus, the Froude number is often defined as *U/Nh* in a stratified fluid flow, where *N*

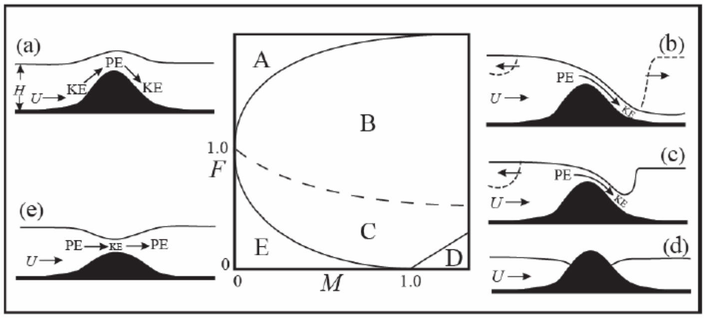


Fig. 3.3: Five flow regimes of the transient one-layer shallow water system, based on the two nondimensional control parameters ($F_o = U/\sqrt{gH}$, $M_c = h_m/H$): (a) supercritical flow, (b) flow with both upstream and downstream propagating jump, (c) flow with upstream propagating jump and downstream stationary jump, (d) completely blocked flow, and (e) subcritical flow. (Lin 2007; Adapted after Baines 1995)

is the Brunt-Vaisala frequency and *h* is the mountain height. Some scientists argued that the physical meaning of *U/Nh* is very different from the Froude number ($F \equiv U/\sqrt{gH}$), thus prefer to use *Nh/U* and called it nondimensional mountain height.

- Several flow regimes are controlled by the Froude number.

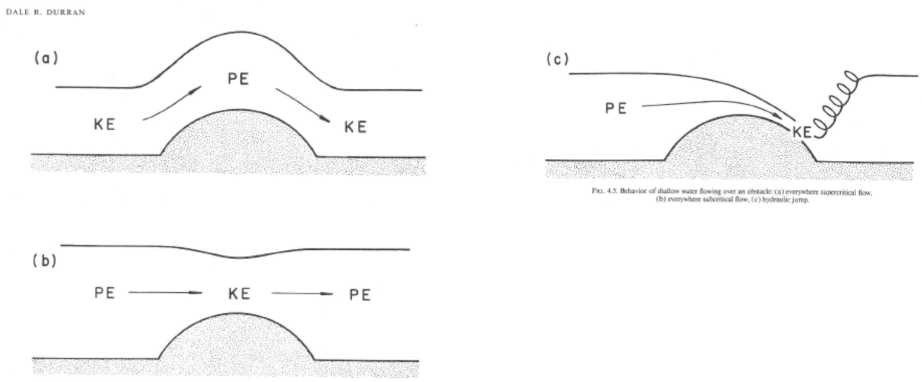


Durran (1990; in Blumen (Ed.), AMS)

### (a) Supercritical Flow ($F > 1$)

If $F > 1$ far upstream, $h' \propto h_s$.

Thus, *h'* increases as $h_s(x)$ increases and the interface bows upwards over the obstacle (Fig. (3.3a)).
Physically, this means that the upstream flow has enough kinetic energy to convert to potential energy and climb over the obstacle. This flow regime is called ***supercritical flow***.

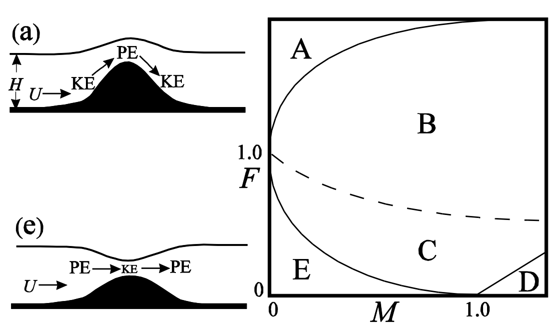


Fig. 3.3 (Lin 2007)

## (e) Subcritical Flow (*F* < *1*)

If $F < 1$, then $h' \propto -h_s$ .

Thus, *h'* decreases as $h_s(x)$ increases.

Physically, this means that a fluid particle does not have enough kinetic energy to climb over the obstacle. In order to surmount the obstacle, the fluid particle needs to draw its potential energy to gain enough kinetic energy (Fig. 3.3e).

Over the peak of the obstacle, the fluid reaches its minimum speed. This flow regime is called ***subcritical flow***. The square of *F* is the ratio of the advection flow speed (*U*) to the shallow water wave or long wave speed ( $\sqrt{gH}$ ).

Thus, when the flow is supercritical ($F > 1$), small disturbance cannot propagate upstream against the flow and any obstacle will produce a purely local disturbance.

When the flow is subcritical ($F<1$), shallow water (long) waves are able to propagate upstream. The steady state effect of this is to increase the layer depth upstream, which increases the potential energy of the flow. The potential energy is then converted to kinetic energy when the fluid surmounts the obstacle. Thus, the fluid reaches its maximum speed and the water surface dips down.

Note that in this type of "steady state" flow, we have

$$\frac{u'}{U} = -\left(\frac{1}{F^2}\right)\frac{h'}{H}. \qquad (3.4.19)$$

The above equation describes the so-called **Bernoulli or Venturi effect**.

- In a transient (unsteady) flow more flow regimes may occur. Dividing Eq. (3.4.17)

$$h' = \left(\frac{U^2}{U^2 - gH}\right)h_s = \frac{h_s}{1 - F^{-2}} \qquad (3.4.17)$$

by $H$ leads to another nondimensional control parameter, $M = h_m/H$. $M$ is also called nondimensional mountain height which measures the nonlinearity of the flow.

Based on $F$ and $M$, there exist 3 other flow regimes in a single-layer transient shallow water system (Long 1970, 1972; Houghton and Kasahara 1968; also see Ch. 3 of Lin 2007 for a brief review), as discussed in the following.

(b) Flow with both upstream and downstream propagating jumps (Fig. 3.3b)

As either $F$ decreases or the non-dimensional obstacle height $M$ increases, the upstream flow is partially blocked and the flow response shifts to the regime in which both an upstream ***hydraulic jump* (*bore*)**, such as the famous Chien-Tang River

Tidal Bore (video) and a downstream jump form and propagate away from the obstacle as time proceeds (Regime b, Fig. 3.3b).

In this case, a transition from subcritical to supercritical states occurs over the peak of the obstacle. Very high velocities are produced along the lee slope since the potential energy associated with the upstream flow is converted to kinetic energy when the fluid passes over and descends along the lee slope of the obstacle.

Eventually, a steady state is established in the vicinity of the obstacle and the free surface shape acquires a *"waterfall-like" profile*.

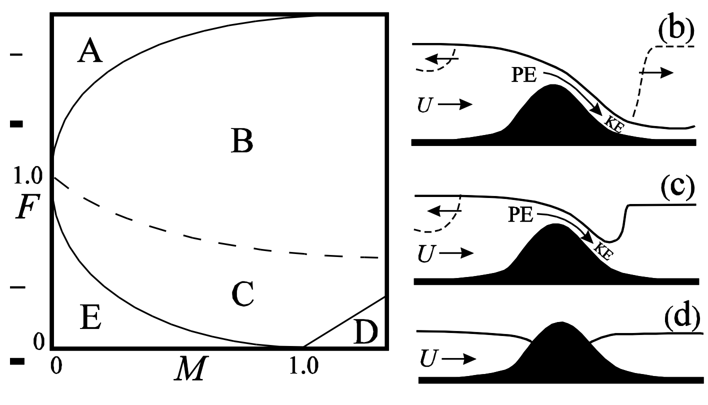


Fig. 3.3 (Lin 2007)

(c) Flow with upstream propagating jump and stationary downstream jump (Fig. 3.3c)

As *F* decreases further, the flow shifts to the regime in which another upstream jump forms and propagates upstream, while the downstream jump becomes stationary over the lee slope due to the weaker advection effect (Regime c, Fig. 4.3c).

*Regimes b and c are characterized by high surface drag and large flow velocities on the lee slope and is referred to as the transitional flow*. This transitional flow has been used to explain the formation of severe downslope wind in the atmosphere (e.g., Long, 1954; Smith, 1985; Durran, 1986; Bacmeister and Pierrehumbert, 1988; see Ch. 5 of Lin 2007 for a review).

(d) Completely blocked flow (Fig. 3.3d).

With a very small $F$ and $M > 1$, the flow response falls into the regime of *completely blocked flow* (Regime d in Fig. 3.3).

Fig. 3.4a show a hydraulic jump formed near Boulder, Colorado, on 11 January 1972 and a sketch (Fig. 4.4b) of regime c which apparently may represent the situation for the 1972 Boulder windstorm. A severe downslope wind over the Front Range to the east of the continental divide reached a value of over 60 $ms^{-1}$. The mechanisms for producing severe downslope winds will be discussed in the chapter of orographically forced flow (Ch. 5). An example of an internal hydraulic jump occurred in the atmosphere is shown in Fig. 3.5.

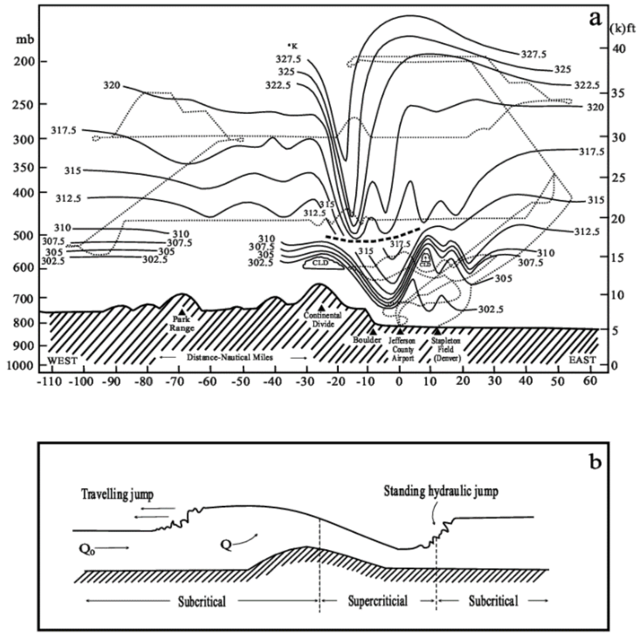


Fig. 3.4: (a) Analysis of potential temperature from aircraft flight data and rawinsondes for the 11 January 1972 Boulder *windstorm*. Aircraft tracks are shown by dashed lines with locations of significant turbulence shown by plus signs. The heavy dashed line separates data taken by the Queen Air aircraft (before 2200 UTC) and from the Saberliner aircraft (after 0000 UTC) (Adapted after Klemp and Lilly 1975). The severe downslope wind reached a value greater than 60 $ms^{-1}$. (b) A sketch of flow Regime c of Fig. 4.3, which may be used to explain the phenomenon associated with (a). Q represents the volume flux per unit width. (Lin 207; Adapted after Turner 1973)


Fig. 4.5: A hydraulic jump in a supercritical airflow over the Sierra Nevada mountain range, made visible by the formation of clouds, and by dust raised from the ground in the turbulent flow behind the jump. (Lin 2007; Photographed by Robert Symons, published in *Comm. Pure and Applied Math*, **20**, no. 2, (review by M. J. Lighthill, @John Wiley and Sons, Inc., 1967).

➢ If the nonlinear terms are considered, then ***wave steepening*** and ***wave overturning*** may occur.

The nonlinear effects on wave steepening may be elucidated by imaging an elevated wave, which is composed of several rectangular blocks with smaller blocks on top of larger blocks. Since the shallow water wave speed is proportional to the layer depth, the speed of fluid particles in the upper layer is higher than that in the lower layer. Thus, the wave front will steepen and possibly overturn. Once overturning occurs, the fluid becomes unstable and turbulence will be induced.

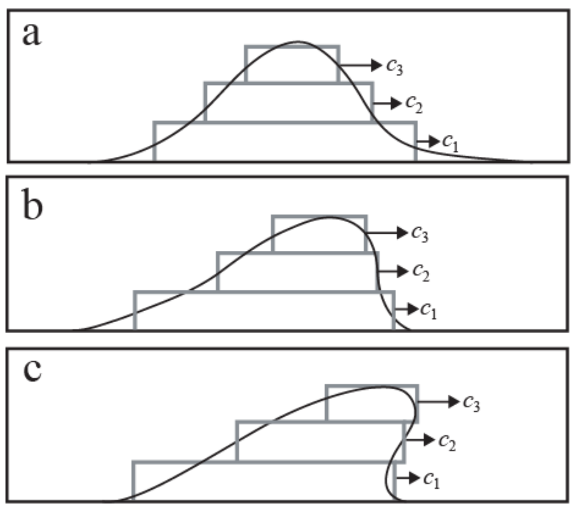


Fig. 3.6: The evolution of an initial symmetric wave, which is imagined to be composed of three rectangular blocks with shorter blocks on top of longer blocks. The wave speeds of these fluid blocks are approximately equal to $c_n = \sqrt{g(H + nh)}$, based on shallow-water theory, where $n$ = 1, 2, and 3, $H$ is the shallow-water layer depth, and $h$ is the height of an individual fluid block. The wave steepening in (b) and wave overturning in (c) are interpreted by the different wave speeds of different fluid blocks because $c_3 > c_2 > c_1$. (Lin 2007 – Mesoscale Dynamics)

➢ Note that for stratified fluid, the Froude number is defined differently:

$$F = U / Nh$$

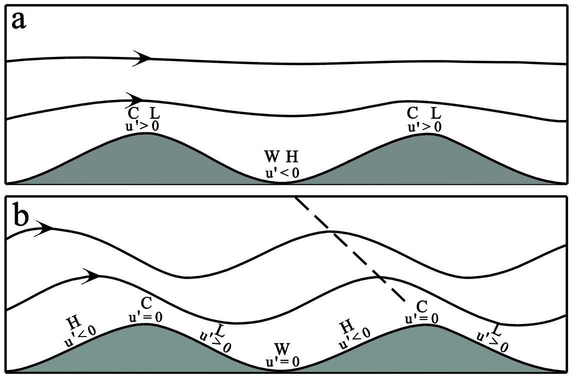


Fig. 5.1: The steady-state, inviscid flow over a two-dimensional sinusoidal mountain when (a) $l^2 < k^2$ ($N < kU$, evanescent waves), where $k$ is the terrain wavenumber (= $2\pi / a$, where $a$ is the terrain wavelength), or (b) $l^2 > k^2$ ($N > kU$, vertically propagating waves). The dashed line in (b) denotes the constant phase line which tilts upstream with height. The maxima and minima of $u'$, $p'$ (H and L), and $\theta'$ (W and C) are also denoted in the figures.

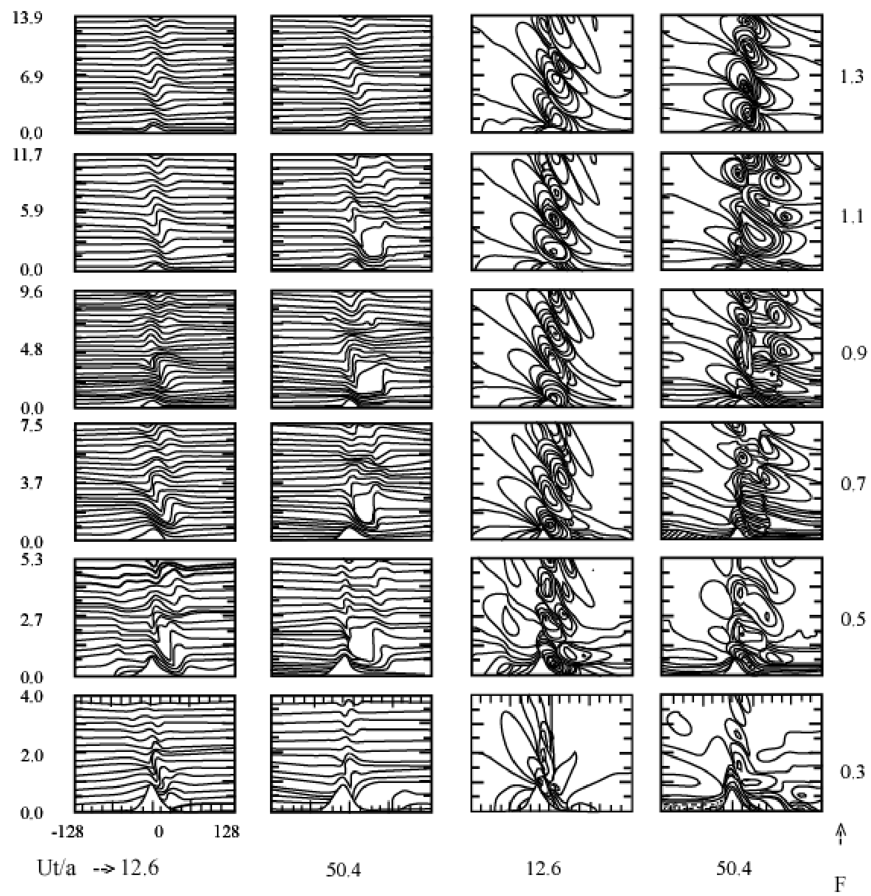


Fig. 6.10: Time evolution of the potential temperature fields (left two columns) and the horizontal velocity fields (right two columns) for a two-dimensional, hydrostatic, uniform flow over a bell-shaped mountain as simulated by a numerical model. The first and third columns correspond to nondimensional time $Ut/a = 12.6$, while the second and fourth columns correspond to $Ut/a = 50.4$. The Froude number ($F = U/Nh$) varies from 0.3 (bottom row) to 1.3 (top row). The dimensional computational domain from $-128$ to $+128\,km$ is plotted against dimensional height ($km$), which corresponds to a constant nondimensional physical domain height of $1.7\lambda_z$ ($\lambda_z = U/Nh$ is the vertical wavelength of hydrostatic waves). (Adapted from Lin and Wang, 1996)

➢ Model Intercomparison for the 1972 Boulder Windstorm during Mesoscale Alpine Program (MAP) (Doyle et al. 2000 Mon. Wea. Rev.)

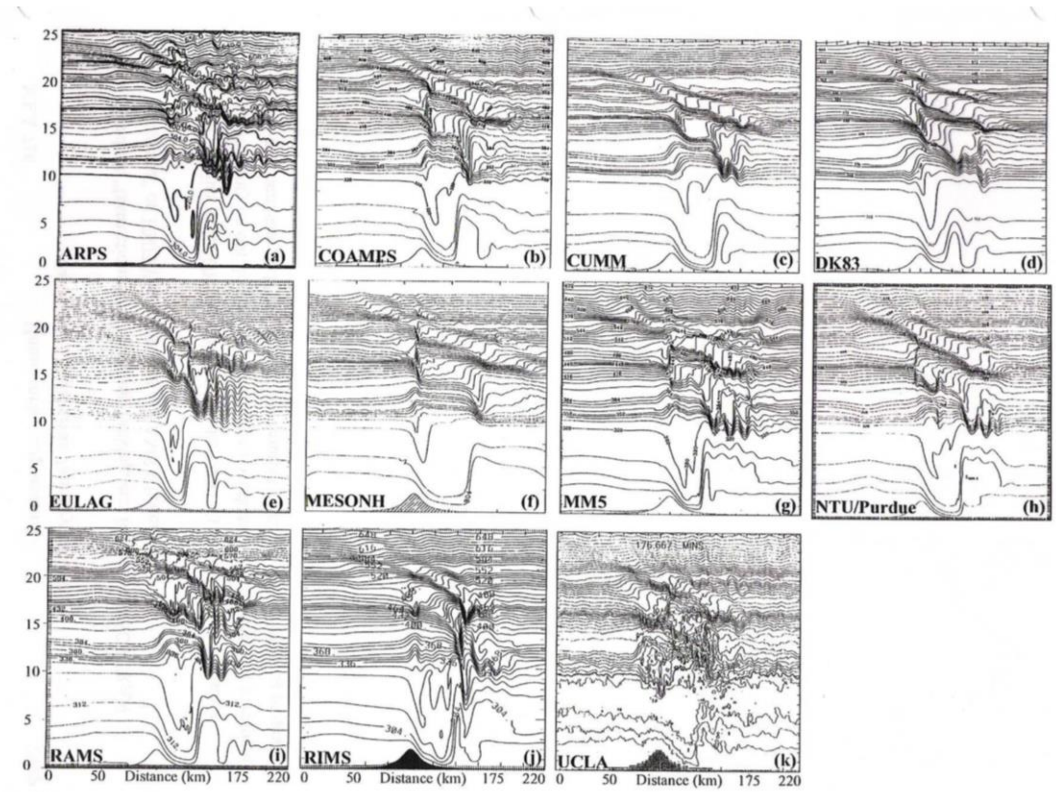


FIG. 3. Vertical cross section of the simulated potential temperature after 3 h for (a) ARPS, (b) COAMPS, (c) CUMM, (d) DK83, (e) EULAG, (f) MESO-NH, (g) MM5, (h) NTU/Purdue, (i) RAMS, (j) RIMS, and (k) UCLA models. The contour interval is 8 K.

- An intercomparison of 2006 T-REX mountain wave simulations (Doyle et al. 2011, Mon. Wea. Rev.)

2818 MONTHLY WEATHER REVIEW VOLUME 139

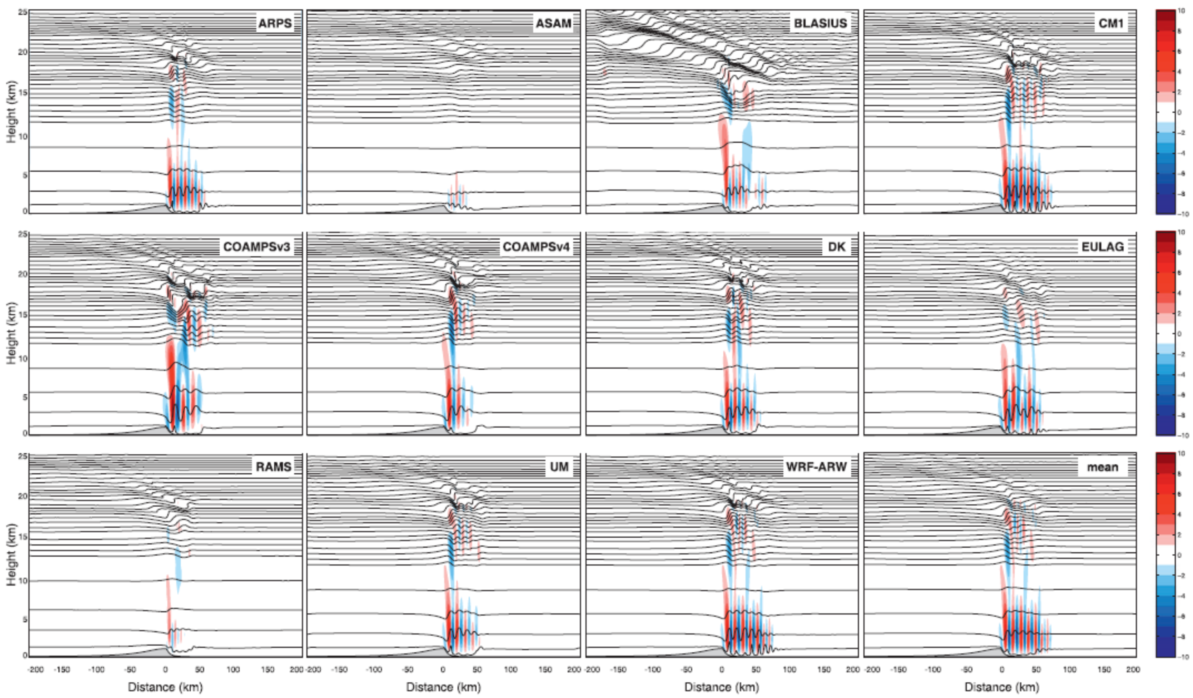


FIG. 4. Vertical velocity (color, interval 1 m $s^{-1}$) and potential temperature (black contours, interval 10 K) for Ex1000_fs case at the final time (4 h) for all models and (bottom right) the mean.